Dalton Transactions

ROYAL SOCIETY OF CHEMISTRY

PAPER

View Article Online
View Journal | View Issue

Cite this: *Dalton Trans.*, 2024, **53**, 15359

The effect of histidine, histamine, and imidazole on electrochemical properties of Cu(II) complexes of Aβ peptides containing His-2 and His-3 motifs†

Aleksandra Tobolska, Agnieszka E. Jabłońska, Aleksandra Suwińska, Urszula E. Wawrzyniak, Wojciech Wróblewski and Nina E. Wezynfeld *

The N-truncation of amyloid beta (Aβ) peptides could lead to peptide sequences with the histidine residue at the second and third positions, creating His-2 and His-3 motifs, known as high-affinity Cu(II) binding sites. In such complexes, the Cu(II) ion is arrested in a rigid structure of a square-planar arrangement of nitrogen donors, which highly limits its susceptibility to Cu(II) reduction. Cu(II) reduction fuels the Cu(II)/Cu(I) redox cycle, which is engaged in the production of reactive oxygen species (ROS). Employing electrochemical techniques, cyclic voltammetry (CV) and differential pulse voltammetry (DPV), together with UV–vis spectroscopy, we showed that low-molecular-weight (LMW) substances, such as imidazole, histamine, and histidine, could enhance the redox activity of Cu(II) complexes of three models of N-truncated Aβ peptides, $A\beta_{4-9}$, $A\beta_{5-9}$, and $A\beta_{12-16}$, identifying three main mechanisms. LMW compounds could effectively compete with Aβ peptides for Cu(II) ions, forming Cu(II)/LMW species, which are more prone to Cu(II) reduction. LMW substances could also shift the equilibrium between the Cu(II)/Aβ species towards the species with higher susceptibility to Cu(II) reduction. Finally, the presence of LMW molecules could promote Cu(I) reoxidation in ternary Cu(II)/Aβ/LMW systems. The obtained results raise further questions regarding the Cu(II) redox activity in Alzheimer's disease.

Received 8th May 2024,
Accepted 17th August 2024

DOI: 10.1039/d4dt01354a

rsc.li/dalton

Introduction

Alzheimer's disease (AD) is the most common neurodegenerative disease worldwide, affecting more than 10% of people aged 65 and above. It causes neuron damage, leading to problems related to memory, thinking, and communication. With AD progression, patients are no longer able to carry out daily activities and require around-the-clock care as the disease spreads through parts of the brain that are responsible for basic functions, such as walking or swallowing, ultimately leading to death.[1]

One of the most well-known hallmarks of AD is fibrils composed of amyloid beta (Aβ) peptides found in the brains of the first diagnosed AD patients,[2,3] which have been an object of extensive research for the last several decades. Soluble Aβ oligomers have been found to be more toxic for neurons than last-stage aggregates,[4] whereas Cu(II) complexes of Aβ peptides have been recognized as active species in catalysing reactive oxygen species (ROS) production.[5] Most studies on Aβ peptides are focused on their full-length form $A\beta_{1-40/42}$, although Aβ peptides are physiologically much more of a heterogenic family consisting of numerous analogues, whose sequences are truncated at N- and C-termini compared to $A\beta_{1-40/42}$.[3,6,7] Furthermore, the amount of truncated Aβ forms could exceed that of $A\beta_{1-40/42}$, such as in the case of $A\beta_{4-42}$, which accounts for more than 60% of Aβ peptides in the brain. The removal of the first three amino acids from the $A\beta_{1-x}$ sequence to create $A\beta_{4-x}$ has tremendous effects on the properties of its Cu(II) complexes. It drastically inhibits the ability of Cu(II) ions to produce ROS by capturing them in a rigid 4N structure of a square-planar complex, where all equatorial sites are occupied by nitrogen donors, namely, the N-terminal amine, two amides, and the imidazole of histidine at the third position in the peptide sequence (His-3)[8] (see the structure of the Cu(II) complex of the model $A\beta_{4-x}$ in Scheme 1). The presence of the His-3 motif in $A\beta_{4-x}$ is crucial for forming such stable Cu(II)/$A\beta_{4-x}$ complexes. A similar structure, but with one vacant position in the equatorial plane, was reported for another Aβ analogue, $A\beta_{5-x}$, which possesses the His residue at the second position (the His-2 motif).[9] This vacant Cu(II) binding site could be filled with external molecules, such as imidazole[9] or phosphates[10,11] (see Scheme 1), but also grants higher suscep-

Chair of Medical Biotechnology, Faculty of Chemistry, Warsaw University of Technology, Noakowskiego 3, 00-664 Warsaw, Poland.
E-mail: Nina.Wezynfeld@pw.edu.pl

† Electronic supplementary information (ESI) available. See DOI: https://doi.org/10.1039/d4dt01354a

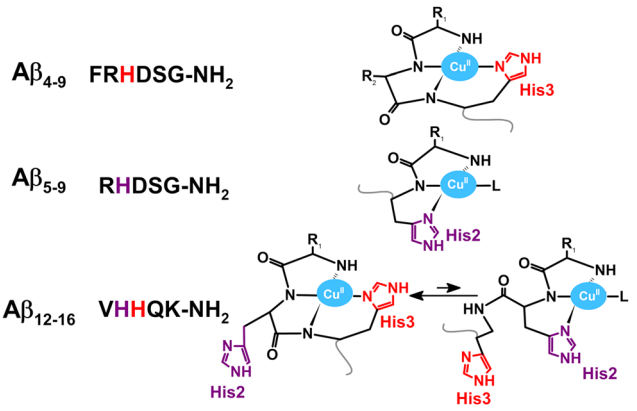

Scheme 1 Sequences of the applied Aβ peptides and the structures of their Cu(II) complexes at pH 7.4. R_1 and R_2 stand for amino acid residues other than the histidine residue. L represents a labile ternary partner, such as water, low-molecular-weight substances, or buffer molecules. The grey curve symbolizes the further part of the peptide chain towards the C-terminus. The structures were prepared based on literature reports.[8,9,16]

tibility to Cu(II) reduction for Cu(II)/Aβ_{5-x} compared to Cu(II)/Aβ_{4-x}.[9–12] Cu(II) reduction followed by Cu(I) reoxidation is the core of the Cu(II)/Cu(I) redox cycle, which fuels ROS production by copper complexes of Aβ peptides.[13] Consequently, the contribution of the 3N Cu(II)/Aβ_{5-x} complex in ROS production is likely higher than that of the 4N Cu(II)/Aβ_{4-x} complex, but still much lower than that of the two-component Cu(II)/Aβ_{1-x} complexes.[5,14]

The hydrolysis of Aβ_{1-x} peptide by neprilysin could lead to the formation of a chimera peptide Aβ_{12-x},[15] containing both His-2 and His-3 motifs, which is able to switch the Cu(II) coordination mode from the 4N characteristic for the His-3 peptides and the main Cu(II)/Aβ_{12-x} species at physiological pH 7.4 to the 3N typical for the His-2 peptides (see Scheme 1). The equilibrium between 4N and 3N complexes for peptides comprising the combined His-2/His3 motif shifts towards the 3N coordination with the pH decreasing[16–18] or in the presence of ternary partners, such as imidazole.[19]

Additionally, the Aβ peptides containing the His-3 and/or His-2 motifs provide much higher Cu(II) affinity compared to the Aβ_{1-x} form. The conditional Cu(II) binding constants given as $\log {}^{c}K_{7.4}$ for the models of Aβ_{4-x} are 13.53–14.18,[8,16] for Aβ_{5-x} are 12.76–12.98,[9] and for Aβ_{12-16} is 14.02.[16] In contrast, the $\log {}^{c}K_{7.4}$ values for Aβ_{1-x} are much lower, in the 10.04–10.43 range,[20] meaning that Cu(II) ions will preferably bind to the N-truncated Aβ peptides containing His-2 and His-3 motifs. In consequence, any alteration of the activity of Cu(II) complexes of those N-truncated Aβ, including their Cu(II) redox activity, would likely impact the overall Cu(II)-related activity, especially that related to ROS production. To study this, we employed three models of N-truncated Aβ peptides possessing His-2 and His3 motifs, namely Aβ_{4-9}, Aβ_{5-9}, and Aβ_{12-16}, with their sequences given in Scheme 1. For a more straightforward interpretation of the results, those models contain only the main Cu(II) binding site of each Aβ form, to which Cu(II) ions are exclusively bound assuming a huge difference between the thermodynamic constants between the first and second Cu(II) binding sites for Aβ_{4-x} and Aβ_{5-x}[8,9] namely of about seven orders of magnitude as calculated for Aβ_{4-x}.[8] The C-termini of the studied model Aβ peptides were blocked by amidation to better represent the properties of the longer forms.

As potential molecules that could alter the properties of the redox properties of Cu(II)/Aβ peptides, we chose physiologically occurring low-molecular-weight (LMW) substances containing an imidazole ring, namely imidazole (Im), histamine (Hstm), and histidine (His). Their structures are provided in Scheme 2. Imidazole is usually investigated as a model for histidine residues in peptides and proteins and has already been shown to act as a ternary partner in Cu(II)/peptide complexes.[9,19,21] Histamine is known as a central neurotransmitter, an immune response modulator, and as a regulator of sleep-wakefulness.[22,23] There are extensive studies on the potential link between histaminergic neurotransmission and the onset of AD. Histamine has been implicated in neuroprotection through antioxidant and anti-inflammatory mechanisms, potentially mitigating neurodegenerative processes related to AD. Histamine's role in modulating neurotransmission, particularly in pathways involving acetylcholine and glutamate, suggests its influence on cognitive function, which is impaired in AD.[24] Moreover, the histamine level and its receptor expression are altered in the brains of AD patients, suggesting potential dysregulation in histaminergic neurotransmission. Elevated histamine levels in the cerebrospinal fluid (CSF) of AD patients have been reported in some studies,[25] but many groups have described lower levels of histamine in various parts of AD brains.[26,27] The exact implications and mechanisms behind these findings require further investigation. It is also worth noting that histaminergic pathways are being explored as potential targets for therapeutic interventions in AD due to their role in neuroprotection and the modulation of cognitive functions. This includes the development of histamine receptor agonists and antagonists aimed at modifying disease progression or alleviating symptoms.[28] Histidine is a precursor of histamine,[22,23] and the changes in its concentration in body fluids could provide insights into histamine metabolism. Indeed, for AD patients, a decline of the His concentration was reported in CSF,[29] but an increase in the urine.[29] Altogether, the literature suggests that LMW molecules could participate in various AD-related processes, their

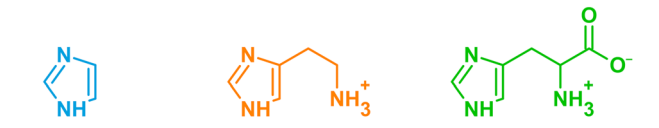

Scheme 2 Structures of the applied low-molecular-weight (LMW) substances.

interactions with Aβ peptides, especially the N-truncated forms and in the complexes with Cu(II) ions, are poorly understood.

We employed two electrochemical techniques, namely cyclic voltammetry (CV) and differential pulse voltammetry (DPV), to describe the effect of LMW molecules on the redox activity of Cu(II) complexes of the Aβ peptides containing the His-2 and His-3 motifs. In both these voltammetric techniques, the potential applied to a working electrode varies in time, and the resulting current is measured. For CV measurements, the working electrode's potential changes linearly up to a given set value and then switches in the opposite direction to reach the initial potential value.[30] Therefore, the CV technique is especially useful for studying processes in which cycling between two oxidation states is important, as is the case for ROS production, which is driven by the redox Cu(II)/Cu(I) cycle.[31–34] For DPV measurements, short pulses are superimposed on the linear changes of the working electrode's potential, and an electrochemical signal is the difference between the current measured before and at the end of each pulse. Consequently, the background current is significantly diminished, increasing the sensitivity of the applied method and allowing for investigations of subtle changes in metal complex structures, for example, resulting from the formation of ternary complexes.[10,11,35,36]

The description of the redox activity for ternary Cu(II)/Aβ/LMW systems is preceded by the results obtained for binary Cu(II) complexes of Aβ peptides containing the His-2 and His-3 motifs, as well as binary systems of Cu(II) ions with the applied LMW substances, *i.e.* imidazole, histamine, and histidine. In addition, we performed a series of UV–vis titrations to see how LMW substances could alter the Cu(II)/Aβ complex structures and the Cu(II) distribution, which could also change their redox activity. During the electrochemical studies on the ternary Cu(II)/Aβ/LMW systems, we focused on Cu(II) reduction due to its high importance in ROS production, but we also included an analysis of Cu(II) oxidation, which could provide valuable information about the complex structure.

Experimental

$CuCl_2$, $Cu(NO_3)_2{\cdot}H_2O$, NaOH, KOH, HCl, KNO_3, HNO_3, imidazole (Im), histamine (Hstm), and histidine (His) were purchased from Sigma-Aldrich (Merck). The concentrations of $CuCl_2$ and $Cu(NO_3)_2$ stock solutions were determined using a molar absorption coefficient of 12.6 M^{-1} cm^{-1} at 816 nm (ref. 19) on a Varian Cary 50 spectrophotometer (Agilent). Amyloid β (Aβ) peptides, namely $A\beta_{4-9}$ FRHDSG-NH_2, $A\beta_{5-9}$ RHDSG-NH_2, and $A\beta_{12-16}$ VHHQK-NH_2, were synthesized according to the Fmoc procedure[37] and obtained from the Institute of Biochemistry and Biophysics PAS (Warsaw, Poland). Their concentrations were determined by UV–vis titrations of the peptide solution in 50 mM HEPES at pH 7.4 with a $CuCl_2$ standard solution, assuming the formation of primarily a 1 : 1 Cu(II) : peptide complex according to the literature.[9,16] The UV–vis spectra for those titrations were recorded in the range of 300–900 nm on a Varian Cary 50 spectrophotometer (Agilent), and the peptide concentration was calculated based on the inflection point of the dependence between the absorbance at the maximum of the d–d band and the Cu(II) concentration in the cuvette.[11,38] For the spectroscopic studies of ternary systems, the 0.45 mM $CuCl_2$/0.50 mM Aβ solution was titrated with the 200 mM solution of the LMW substance, and the UV–vis spectra were recorded in the range of 250–900 nm on a Varian Cary 50 spectrophotometer (Agilent) at least six times to confirm the equilibrium of the system. For His/Cu(II)/$A\beta_{4-9}$, samples of various His concentrations were prepared separately, about 18 h before the measurements, to ensure that equilibrium was achieved in all samples. To avoid the formation of additional ternary species, we did not use an external buffer. The pH value of 7.4 was maintained by adding small amounts of concentrated KOH or HCl solutions as needed.

For electrochemical measurements, we employed a three-electrode cell containing a glassy carbon electrode (GCE, BASi, ∅ = 3 mm) as the working electrode, Ag/AgCl 3 M NaCl as the reference (MINERAL, Poland), and platinum wire as the counter electrode (MINERAL, Poland). An electrolytic bridge filled with 100 mM KNO_3 separated the reference electrode from the working solution. The glassy carbon electrode was sequentially polished with 1.0 μm and 0.3 μm alumina powders on a polishing cloth, followed by 1 min ultrasonication in deionized water. All the electrochemical measurements were carried out in 100 mM KNO_3 at room temperature under an argon atmosphere using a CHI 1030 potentiostat (CH Instrument, TX, USA). The changes in the electrochemical signals of the studied ternary systems, especially His/Cu(II)/$A\beta_{4-9}$, were checked over several hours. The pH was adjusted by adding small amounts of concentrated KOH or HNO_3 solutions and controlled using a SevenCompact pH meter (Mettler-Toledo) with an InLab Micro Pro combination pH electrode (Mettler-Toledo). During the cyclic voltammetry (CV) measurements, the scan rate was 100 mV s^{-1}, whereas, for the differential pulse voltammetry (DPV) measurements, the pulse amplitude was 50 mV and the pulse time was 100 ms.

Results and discussion

Electrochemical properties of Cu(II)/$A\beta_{4-9}$, Cu(II)/$A\beta_{5-9}$, and Cu(II)/$A\beta_{12-16}$ complexes

We started with electrochemical studies on the redox properties of Cu(II) complexes of three Aβ forms, namely $A\beta_{4-9}$, $A\beta_{5-9}$, and $A\beta_{12-16}$. The CV and DPV curves registered at pH 7.4 are given in Fig. 1, while the electrochemical parameters for the main coordination modes are provided in Table 1 and Table S1† for the CV and DPV results, respectively. All the measurements were performed using a slight excess of the peptide over Cu(II), which was in line with the literature data on the main 1 : 1 stoichiometry observed for Cu(II) complexes of the peptides containing the His-2 or His-3 motif.[8,9,16,17,39]

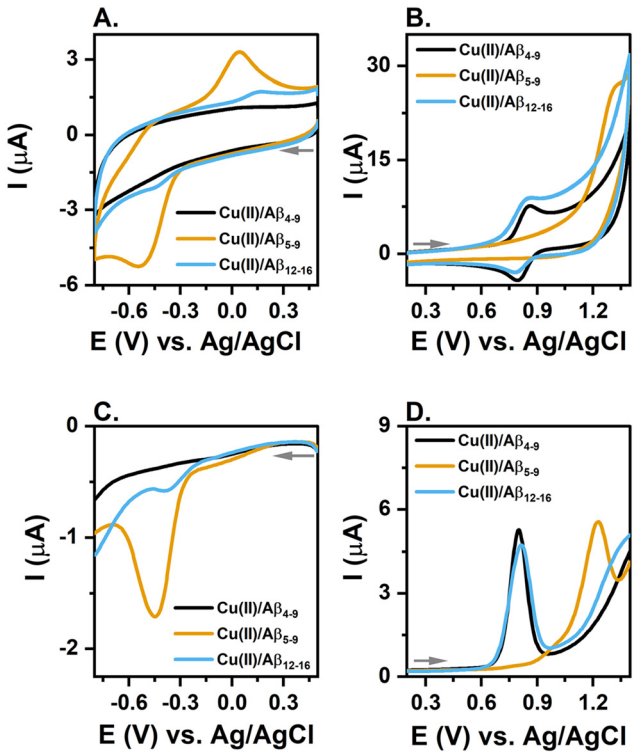

Fig. 1 CV (A and B) and DPV (C and D) curves recorded scanning towards more negative (A and C) or more positive (B and D) potential values for 0.45 mM Cu(II) and 0.50 mM Aβ peptides in 100 mM KNO_3, pH 7.4.

This approach also allowed us to reduce the amount of highly redox-active Cu(II) ions not bound to the peptide.[40]

No signals were observed for Cu(II)/$Aβ_{4-9}$ scanning towards negative potential values up to −0.8 V *vs.* Ag/AgCl during the CV (Fig. 1A) and DPV (Fig. 1C) measurements. A similar effect was previously reported for another model of $Aβ_{4-x}$, namely $Aβ_{4-16}$.[8,14,41] Such inertness to Cu(II) reduction resulted from the formation of stable and rigid complexes by $Aβ_{4-x}$, in which all the equatorial Cu(II) binding sites were occupied by nitrogen donors of the N-terminal amine, two amides, and the His-3 imidazole, creating the 4N coordination mode.[8,16] Esmieu *et al.* showed that reducing Cu(II) in such a complex requires highly negative potential values around −1.5 V *vs.* Ag/AgCl,[41] which is far beyond physiological conditions,[42] and therefore was not used in our study.

Cu(II) reduction for the complex of the next studied N-truncated Aβ form, $Aβ_{5-9}$, was noticed at −0.54 V *vs.* Ag/AgCl from the CV curves (Fig. 1A). This peptide comprised the His-2 motif, in which nitrogen donors occupy the three equatorial binding sites at pH 7.4, namely the N-terminal amine, the amide, and the His-2 imidazole, forming the 3N coordination mode. A water molecule or other loosely bound ligands could cover the fourth site.[10] The relatively large difference between the signal assigned to Cu(II) reduction and, in the reverse scan, Cu(I) oxidation (see Fig. 1A and Table 1) suggested a substantial reorganization of the complex structure during the transition between the Cu(II) and Cu(I) oxidation states, which aligns with the square-planar arrangement of the donors in the Cu(II) complex and the expected linear structure of the Cu(I) complex. These results agree with our previous studies on Cu(II)/$Aβ_{5-x}$,[9,10] as well as with literature data for other Cu(II) complexes of His-2 peptides.[11,35,43]

Signals assigned to the Cu(II)/Cu(I) redox cycle for the Cu(II)/$Aβ_{12-16}$ complex were observed at values similar to Cu(II)/$Aβ_{5-9}$ potential values (Fig. 1A and C), but with diminished intensities. The $Aβ_{12-16}$ peptide contains both the His-2 and His-3 motifs, which supports the formation of 3N- and 4N-type complexes.[16] At pH 7.4 and an almost equimolar Cu(II) and peptide amount, the 4N coordination prevailed, utilizing about 99.8% of the Cu(II) ions. The remaining 0.2% of Cu(II) (approximately 1 μM) was bound in the 3N complexes (see the Cu(II) species distribution for $Aβ_{12-16}$ in Table S2†), justifying the presence of the Cu(II) reduction signal characteristic for the 3N complex. In more acidic conditions, the molar fraction of the 3N coordination increased[16] (see Table S2†), corresponding to higher intensities of the signals, as shown in Fig. S1.† However, the acidification could also lead to the presence of the Cu(II) ions not bound to the peptide, which undergo reduction at less negative potential values than for 3N complexes around 0.0 V *vs.* Ag/AgCl (see the CV curves at pH 4.5 in Fig. S1†).

Table 1 Electrochemical potential values related to the Cu(II) redox processes for 4N and 3N coordination modes of Cu(II)/Aβ complexes calculated based on CV curves at 100 mM KNO_3 as the mean of at least three independent repetitions with standard deviation values as the last digit given in parentheses

		E (V) *vs.* Ag/AgCl					
		CV					
Cu(II) complexes	Coordination	Cu(II)/Cu(I)	Cu(I)/Cu(II)	$\Delta E_{Cu(II)/Cu(I)}$	Cu(II)/Cu(III)	Cu(III)/Cu(II)	$\Delta E_{Cu(II)/Cu(III)}$
Cu(II)/$Aβ_{4-9}$	4N	n.d.	n.d.	—	0.87(1)[a]	0.80(1)[a]	0.07(1)[a]
Cu(II)/$Aβ_{5-9}$	3N	−0.54(1)[a]	0.04(2)[a]	0.58(2)[a]	1.32(1)[a]	n.d.	—
Cu(II)/$Aβ_{12-16}$	3N	−0.46(1)[a,c]	0.15(2)[a] 0.27(3)[c]	0.60(1)[a] 0.74(2)[c]	1.29(1)[b]	n.d.	—
	4N	n.d.	n.d.	—	0.89(1)[a]	0.80(1)[a]	0.09(1)[a]

n.d. not detected. [a] Based on the measurements at pH 7.4. [b] Based on the measurements at pH 3.8–4.5. [c] Based on the measurements at pH 4.5–5.0.

The presence of two adjacent His residues in the $A\beta_{12-16}$ sequence should also stabilize the Cu(I) oxidation state. However, we did not notice the expected bigger separation between the Cu(II) reduction and Cu(I) oxidation potentials (ΔE) for $A\beta_{12-16}$ (containing bis-His motif) compared to $A\beta_{5-9}$ (containing only the His2 residue) at pH 7.4. But, this appeared at a more acidic pH of around 5.0 (see Table 1 and Table S1†). Cu(I) stabilization was reported previously for AHH in relation to an AH complex at pH 6.2.[17] The lack of such effect in the presence of $A\beta_{12-16}$ at pH 7.4 likely resulted from the very weak interaction between Cu(I) and $A\beta_{12-16}$ during the electrochemical measurements at this pH due to: (i) the low amount of copper ions participating in the electrochemical reactions (around 1 μM Cu(II) was in the 3N complex and could be reduced to Cu(I) at pH 7.4) and (ii) the moderate Cu(I) affinity constant for this type of peptides (around 2×10^6 M^{-1} by analogy to $A\beta_{11-16}$, EVHHQK).[41] As described above, at more acidic conditions, the amount of Cu(II) ions involved in the 3N complex was higher (Table S2†); in consequence, more Cu(II) ions were reduced to Cu(I) (see Fig. S1†), facilitating the interaction between Cu(I) and $A\beta_{12-16}$ and shifting the Cu(I) re-oxidation potential towards higher values (see Fig. S1†).

Analysing the Cu(II) oxidation signals at pH 7.4, which were obtained when scanning towards more positive potential values during the CV (Fig. 1B) and DPV measurements (Fig. 1D), we noticed a high resemblance between the redox activity of Cu(II)/$A\beta_{4-9}$ and Cu(II)/$A\beta_{12-16}$, both showing a predominant contribution of the 4N complex at this pH value. For the CV curves, the Cu(II) oxidation was noticed at around 0.9 V *vs.* Ag/AgCl with the corresponding Cu(III) reduction signals at 70–90 mV lower potential values. These results are consistent with literature data on short models of $A\beta_{4-x}$.[14] In contrast, Cu(II) oxidation for the 3N complex of Cu(II)/$A\beta_{5-9}$ occurred at higher potentials, around 1.3 V *vs.* Ag/AgCl. This process was irreversible as no signals were noticed in the reverse scan and was likely associated with the oxidation of the His residue by reactive Cu(III) species at high potentials. The characteristic signals for Cu(II) oxidation for the 3N complex were also observed for Cu(II)/$A\beta_{12-16}$, but at acidic conditions, as shown in Fig. S2 and S3B.† In agreement with the results for the 3N complex of $A\beta_{5-9}$, the Cu(II) oxidation for the 3N complex $A\beta_{12-16}$ was also irreversible (see Fig. S3†).

Electrochemical properties of Cu(II)/His, Cu(II)/Hstm, and Cu(II)/Im binary systems

In the next step, we performed measurements for binary systems of Cu(II) ions and LMW substances, including histidine (His), histamine (Hstm), and imidazole (Im). The Cu(II) complexes of those substances could contain more than one ligand molecule per Cu(II) ion, and their stability highly depends on the ligand excess, as observed during the UV–vis titration with those LMW substances (Fig. S4†) and as described in the literature.[44–46] We also demonstrated that the LMW : Cu(II) ratio also highly affects the electrochemical response, especially the Cu(II)/Cu(I) cycle (Fig. S5 and S6†). Therefore, we mainly applied 5.0 mM concentration of LMW substances in our measurements (about 11-fold excess of the LMW compound over Cu(II)) to saturate the copper binding sites by the given LMW molecules. Comparisons of the respective CV and DPV curves for all the Cu(II)/LMW binary systems are given in Fig. 2, whereas the electrochemical parameters associated with the Cu(II)/Cu(I) cycle are provided in Table 2.

Cu(II) reduction was highly facilitated in the presence of imidazole, as indicated by its potential value of 0.08 V *vs.* Ag/AgCl and the relatively high reversibility of this process due to the proximity of the Cu(II) reduction and Cu(I) oxidation signals (see Table 2 and Fig. S6†). Cu(II) ions are more resistant to reduction when they form complexes with ligands containing additional groups attached to the imidazole ring, such as histamine with an amine group or histidine with amine and carboxyl groups. In those cases, the Cu(II) reduction potential was shifted to more negative values and was more separated from the Cu(I) oxidation signal (see Table 2). Note that the decrease in the Cu(II) reduction potential value and lower reversibility of the Cu(II)/Cu(I) cycle were highly associated with the increase of the Cu(II) complex stability in the order imidazole < histamine < histidine (the complex stability was estimated based on values of the negative logarithms of Cu(II) ions not bound to the ligand, *i.e.* pCu values of 3.8 < 9.80 < 13.15, respectively).[19,45,47]

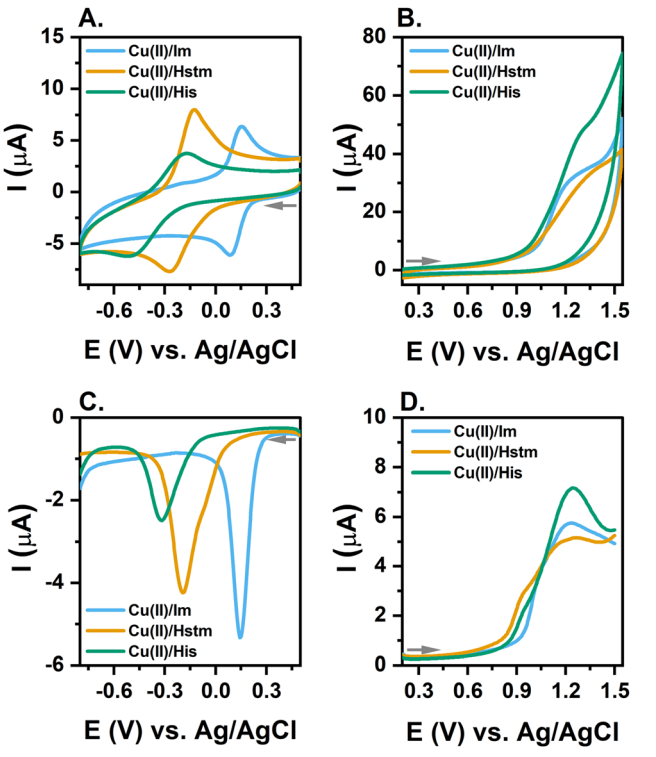

Fig. 2 CV (A and B) and DPV (C and D) curves recorded scanning towards more negative (A and C) or more positive (B and D) potential values for 0.45 mM Cu(II) and 5.00 mM histidine (His), histamine (Hstm), and imidazole (Im) in 100 mM KNO_3, pH 7.4.

Table 2 Electrochemical potential values related to the Cu(II)/Cu(I) cycle for the binary systems of Cu(II) and low-molecular-weight substances (LMW): imidazole (Im), histamine (Hstm), and histidine (His) calculated based on CV and DPV curves at pH 7.4 and 100 mM KNO_3 as the mean of at least three independent repetitions with standard deviation values as the last digit given in parentheses

	E (V) *vs.* Ag/AgCl			
	CV			DPV
Binary Cu(II)/LMW system	Cu(II)/Cu(I)	Cu(I)/Cu(II)	$\Delta E_{Cu(II)/Cu(I)}$	Cu(II)/Cu(I)
0.45 mM Cu(II)/5.0 mM Im	0.08(2)	0.14(2)	0.07(1)	0.14(2)
0.45 mM Cu(II)/5.0 mM Hstm	−0.29(2)	−0.13(2)	0.16(2)	−0.20(2)
0.45 mM Cu(II)/5.0 mM His	−0.48(2)	−0.22(4)	0.27(5)	−0.34(3)

In contrast, scanning towards more positive values, the main signal observed in the CV and DPV curves for all the Cu(II)/LMWs systems appeared at a similar potential of about 1.25 *vs.* Ag/AgCl (Fig. 2B and D). Such a picture is characteristic of the irreversible electrochemical oxidation of the imidazole ring in the imidazole-containing substances, often leading to the adsorption of a polymer-like product on the electrode.[48–50] The presence of Cu(II) likely slightly affects this process as the intensities of the oxidation signals registered for imidazole and histamine were decreased upon Cu(II) addition, while the peak of the histidine oxidation was shifted by about 50 mV, as shown in Fig. S7.†

Spectroscopic analysis of the ternary Cu(II)/Aβ/LMW systems

The investigation of the effects of the LMW substances on the electrochemical properties of Cu(II)/Aβ complexes was performed by spectroscopic characterization of the ternary systems. The UV–vis spectra for the titration of Cu(II)/Aβ complexes with the studied LMW substances, together with the control spectra of the Cu(II)/LMW complexes, are provided in Fig. 3.

No significant changes were observed upon the addition of imidazole to the Cu(II)/$A\beta_{4-9}$ complex (Fig. 3A). This aligns with the theoretical calculations on the Cu(II) distribution between Aβ and LMW substances given in Table S3.† Considering the formation of exclusively binary complexes, imidazole is unlikely to compete for Cu(II) ions with $A\beta_{4-9}$ as well as with $A\beta_{5-9}$ or $A\beta_{12-16}$. However, for ternary systems comprising imidazole and $A\beta_{5-9}$ or $A\beta_{12-16}$, a d–d band shift was noticed towards shorter wavelengths for the $A\beta_{5-9}$ system (Fig. 3D) and towards longer wavelengths for the $A\beta_{12-16}$ system (Fig. 3G). Such spectral fingerprints are characteristic of the formation of ternary complexes with peptides containing the His-2 motif[9,10,21,51,52] and combined His-2 and His-3 motifs,[19] respectively. In the first case, imidazole fulfils the vacant space in the equatorial plane of the 3N Cu(II) complex of the His-2 peptide ($A\beta_{5-9}$), resulting in a blue-shift of the d–d band.[9] For the Cu(II) complex of the His-2/His-3 peptide (such as $A\beta_{12-16}$), with the predominant 4N coordination at pH 7.4, the formation of the ternary complex with imidazole required a switch to the 3N Cu(II)/peptide coordination, which makes the fourth site in the equatorial plane available for the interaction with imidazole.[19] The internal rearrangement of the Cu(II) complexes of His-2/His-3 peptides from the 4N to 3N coordination, followed by the formation of a ternary 3N + 1N complex, was in line with the red-shift of the registered d–d band for the Im/Cu(II)/$A\beta_{12-16}$ system (Fig. 3G).

In contrast, comparison of the Cu(II) affinity of the studied N-truncated Aβ peptides and histidine (see Table S3†) suggested potential competition between those molecules for Cu(II) ions. Indeed, we observed a gradual conversion in the UV–vis spectra in the course of the measurements for all the studied Cu(II)/Aβ complexes with histidine (Fig. 3C, F and I), as expected for the transfer of Cu(II) ions from Aβ to histidine. Note that such transfer could last longer than the mixing time due to the rigid structure of the studied Cu(II)/Aβ complexes. For example, monitoring the changes of the UV–vis spectra upon the addition of histidine to the Cu(II)/Aβ complexes (Fig. S8,† final reagent concentrations of 5.0 mM His/0.45 mM Cu(II)/0.50 mM Aβ), we demonstrated that it took about 3 h to achieve equilibrium for the $A\beta_{4-9}$ system, while it took about 15 min for $A\beta_{12-16}$, and less than 3 min (time of the reagent mixing and registering the spectrum) for $A\beta_{5-9}$ (see the kinetics in Fig. S9†). The relatively slow withdrawal of Cu(II) ions from $A\beta_{4-9}$, the peptide containing the His-3 motif, agreed with the previously reported results on the interaction of Cu(II) complexes of $A\beta_{4-x}$ with metallothionein-3, EDTA, Cys, and GSH.[53–55] The much faster reactivity of Cu(II)/$A\beta_{12-16}$ with GSH compared to Cu(II)/$A\beta_{4-9}$ has also been reported.[55] On the other hand, the His-2 motif, which facilitates Cu(II) transfer to the histidine compared to the His-3 motif, also promotes the formation of Cu(II)-peptide complexes, as reported by Gonzalez *et al.*; the slowest rate of the Cu(II) binding was noted for the His-3 peptide AAH, faster than for the His-2/His-3 peptide AHH, and the fastest for AH.[56] Thus, the presence of combined His-2 and His-3 motifs in the peptide sequence significantly facilitate both the association and dissociation of their Cu(II) complexes compared to those with the His-3 motif alone. The spectra collected in Fig. 3 are the final ones after reaching equilibrium. Besides the ternary system compromising histidine and $A\beta_{4-9}$ or $A\beta_{12-16}$, we did not notice any significant time-related changes upon mixing in the reagents.

A more detailed analysis of the spectral changes during the titrations of Cu(II)/Aβ complexes with histidine is given in Fig. S10† and showed that the increase in the intensity of the d–d band characteristic for Cu(II)/His complexes was less pro-

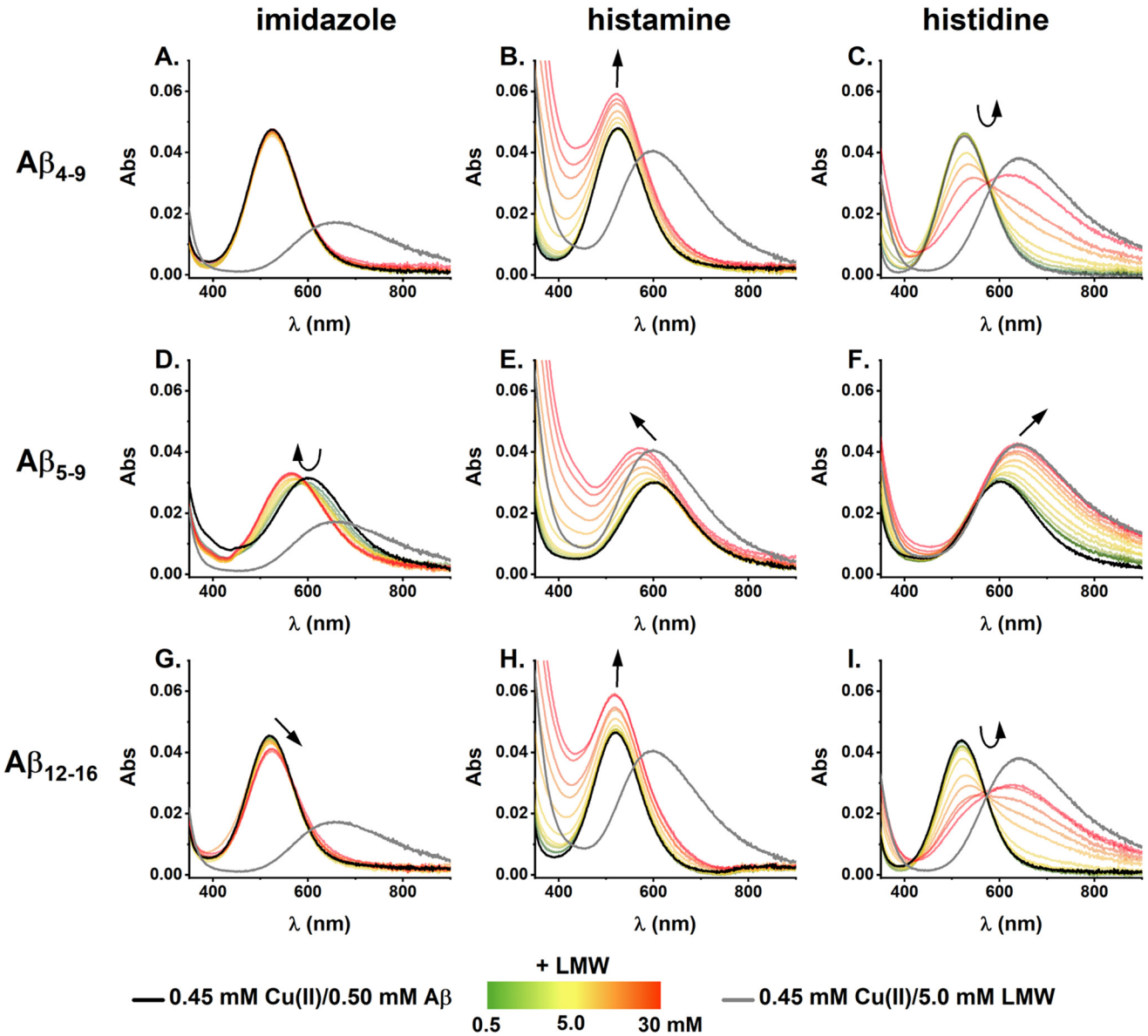

Fig. 3 UV–Vis spectra for the titration of 0.45 mM Cu(II)/0.50 mM Aβ peptides, $A\beta_{4-9}$ (A–C), $A\beta_{5-9}$ (D–F), and $A\beta_{12-16}$ (G–I) with LMW substances, imidazole (A, D, G), histamine (B, E, H), and histidine (C, F, I), in the 0.50–30 mM concentration range coded with the gradient colors from green (0.50 mM LMW) to red (30 mM LMW). The black line refers to the initial spectrum of 0.45 mM Cu(II)/0.50 mM Aβ peptide, whereas the grey line refers to the control spectrum of 0.45 mM Cu(II)/5.0 mM LMW substance. The titration was performed at pH 7.4. The arrows represent the direction of spectral changes during the titrations.

nounced for $A\beta_{5-9}$ and $A\beta_{12-16}$ than expected from theoretical calculations, where we assumed only the formation of binary Cu(II)/Aβ and Cu(II)/His complexes. For Cu(II)/$A\beta_{5-9}$/His, such analysis could be hampered by the proximity of the d–d bands of the Cu(II)/$A\beta_{5-9}$ and Cu(II)/His binary complexes (Fig. 3F). But even if the whole theoretical spectra were analyzed (data not shown), the theoretical amount of binary Cu(II)/LMW complexes would still be higher than the experimental ones. This could be explained by the participation of the intermediate species, likely the ternary complex Cu(II)/Aβ/His, in transferring Cu(II) ions from $A\beta_{5-9}$ and $A\beta_{12-16}$ to histidine, which is in line with their ability to form ternary complexes with those His-2 peptides.

The interpretation of the results obtained during the titrations with histamine was even more challenging due to the increase in absorbance at lower wavelengths observed at higher histamine concentrations, which also affected the signal of the d–d band of the Cu(II)/Aβ complexes (Fig. 3B, E and H). For example, a similar increase of the d–d band intensity, but without the spectral shift, was noted for the system with $A\beta_{4-9}$ and $A\beta_{12-16}$ (Fig. 3B and H). Theoretical calculations indicated that histamine would not effectively compete for Cu(II)

ions with those peptides (Table S3†), and as shown for the ternary system Im/Cu(II)/Aβ$_{4-9}$ (Fig. 3A), the 4N complexes of the His-3 motif were not prone to form ternary complexes with the external molecules. Therefore, there was no clear evidence confirming the formation of ternary complexes between histamine and Cu(II)/Aβ$_{4-9}$ or Cu(II)/Aβ$_{12-16}$. On the other hand, the titration of Cu(II)/Aβ$_{5-9}$ with histamine was associated with a blue-shift of the d–d band characteristic for the ternary Cu(II) complexes of the His-2 peptides. Based on the theoretical calculations given in Table S3,† Cu(II) transfer from Aβ$_{5-9}$ to histamine is also possible, but considering practically the same position of the d–d bands for Cu(II)/Aβ$_{5-9}$ and Cu(II)/Hstm (about 600 nm), but higher intensity of the latter, such a reaction should be manifested mostly as an increase in A_{600} intensity but without a shift. Despite the fingerprint of the ternary Hstm/Cu(II)/Aβ$_{5-9}$ complex being clearly spotted, we could not exclude the formation of the binary Cu(II)/Hstm species, as their spectral signals are very alike.

Following the changes at the d–d bands that could be assigned to the ternary complexes, Cu(II)/Aβ$_{5-9}$ with imidazole and histamine, and Cu(II)/Aβ$_{12-16}$ with imidazole, given in Fig. S11,† we could conclude that their stability decreased in the order Im/Cu(II)/Aβ$_{5-9}$ > Im/Cu(II)/Aβ$_{12-16}$ > Hstm/Cu(II)/Aβ$_{5-9}$. The four-times weaker affinity of imidazole to Cu(II)/Aβ$_{12-16}$ than to Cu(II)/Aβ$_{5-9}$ aligned perfectly with the results obtained for the interaction of imidazole with Cu(II)/AHH and Cu(II)/AH, respectively.[19] The lowest stability of the ternary system of Hstm/Cu(II)/Aβ$_{5-9}$ could be due to the more extensive structure and higher positive charge of histamine compared to imidazole, which could impede the formation of ternary species. However, the error in the K_a value calculated for this system was likely higher than obtained from the fitting due to the mentioned increase in the basal signal at high histamine concentrations.

Electrochemistry studies of the ternary Cu(II)/Aβ/LMW systems

Cu(II) reduction in the ternary Cu(II)/Aβ/LMW systems. The CV curves for the ternary systems Cu(II)/Aβ/LMW recorded in the potential range typical for the Cu(II)/Cu(I) cycle and the respective signals for binary systems Cu(II)/Aβ and Cu(II)/LMW are shown in Fig. 4. The analogous DPV curves are given in Fig. S12.† For clarity, those comparisons represent the measurements for 0.45 mM Cu(II), 0.50 mM Aβ peptides, and 5.0 mM LMW substance concentrations. The electrochemical results in the 0.5–5.0 mM concentration range of LMW compounds are available in the ESI, Fig. S13† for the CV curves, and Fig. S14† for the DPV curves.

We did not notice any significant signal for Cu(II) reduction upon imidazole addition to Aβ$_{4-9}$, as shown in Fig. 4A, S12A, S13A, and S14A.† Thus, imidazole did not induce the reduction of Cu(II) ions engaged in the rigid structure of the complex with the His-3 peptide. This aligns with the theoretical calculations on the Cu(II) distribution between Aβ and LMW substances given in Table S3† and the results of the respective spectroscopic titrations (Fig. 3A). On the other hand, imidazole caused a slight alteration in the shape of the electrochemical curves for Cu(II)/Aβ$_{5-9}$ (especially for the CV measurements around −0.55 V, Fig. 4D, S13D†) and a current increase for the signals related to Cu(II) reduction and Cu(I) oxidation for Cu(II)/Aβ$_{12-16}$ (Fig. 4G, S12G, S13G and S14G†). In both cases, *i.e.* for Cu(II)/Aβ$_{5-9}$ and Cu(II)/Aβ$_{12-16}$, such effects were likely primarily associated with the formation of the ternary 3N + 1 complex. However, whereas the "weak redox-active" 3N complex was already a major species for Cu(II)/Aβ$_{5-9}$ at pH 7.4, the major coordination mode for Cu(II)/Aβ$_{12-16}$ at the same condition was the "redox-inert" 4N complex, which, in the presence of imidazole, was forced to convert to the 3N coordination and finally to the 3N + 1N complex. As the amount of "weak redox-active" 3N complex increased for the Im/Cu(II)/Aβ$_{12-16}$ system, we observed a current rise for the signals for the Cu(II)/Cu(I) cycle, whereas the completion of the equatorial plane of the 3N complex by the labile imidazole molecule for the Im/Cu(II)/Aβ$_{5-9}$ system was associated with a slight alteration of the Cu(II) reduction signal.

Similarly to the Cu(II)/Aβ$_{4-9}$/Im ternary system, we did not notice changes upon the addition of histamine to Cu(II)/Aβ$_{4-9}$ (Fig. 4B, S12B, S13B and S14B†), whereas evident signals related to the Cu(II)/Cu(I) cycle appeared for Cu(II)/Aβ$_{4-9}$/His (Fig. 4C, S12C, S13C and S14C†). As shown in the spectroscopic studies, this could be explained by the competitive binding of Cu(II) ions by histidine from Aβ$_{4-9}$ (Fig. 3C), whereas histamine could barely compete with Aβ$_{4-9}$ for Cu(II) under analogous conditions (Fig. 3B, Table S3†).

Histidine could also effectively withdraw Cu(II) ions from Aβ$_{5-9}$ and Aβ$_{12-16}$, as confirmed by the spectroscopic results, while histamine could theoretically remove Cu(II) ions from Aβ$_{5-9}$ (see Table S3†). However, as mentioned above, for the systems involving His-2 peptides, such as Aβ$_{5-9}$ and Aβ$_{12-16}$, another scenario was also possible: the formation of ternary complexes. The electrochemical indication of the former process, *i.e.* the competitive Cu(II) binding to LMW, could be observed for Cu(II)/Aβ$_{5-9}$/Hstm with the current rise at potentials typical for the reduction of Cu(II) ions bound to histamine (see the DPV curves in Fig. S12E†). On the other hand, the alteration in the signal shape for Cu(II) reduction (Fig. 4E) was analogous to those registered for the ternary complex of the Im/Cu(II)/Aβ$_{5-9}$ system (Fig. 4D). Thus, both reactions, *i.e.* the competitive binding of Cu(II) ions by histamine and the formation of the ternary Hstm/Cu(II)/Aβ$_{5-9}$ complex, could occur for this system. It was more problematic to distinguish those signals for the systems comprising histidine and the His-2 peptides, as the Cu(II) reduction potentials for the 3N Cu(II)/peptide complex were close to those of the Cu(II)/His complexes (see Fig. 4F, I, S12F, S12I† and Tables 1, 2, and Table S1†). However, the barely noticeable impact of histamine on the Cu(II) reduction in the system involving Cu(II)/Aβ$_{12-16}$ (Fig. 4H) suggested that the more extensive structure of LMW molecules and more positive charge of histamine compared to imidazole could impede the formation of the ternary complexes. Steric hindrance could be expected to be even greater in the case of histidine, but the negative charge of its carboxylic acid should be in favour of the interaction between the

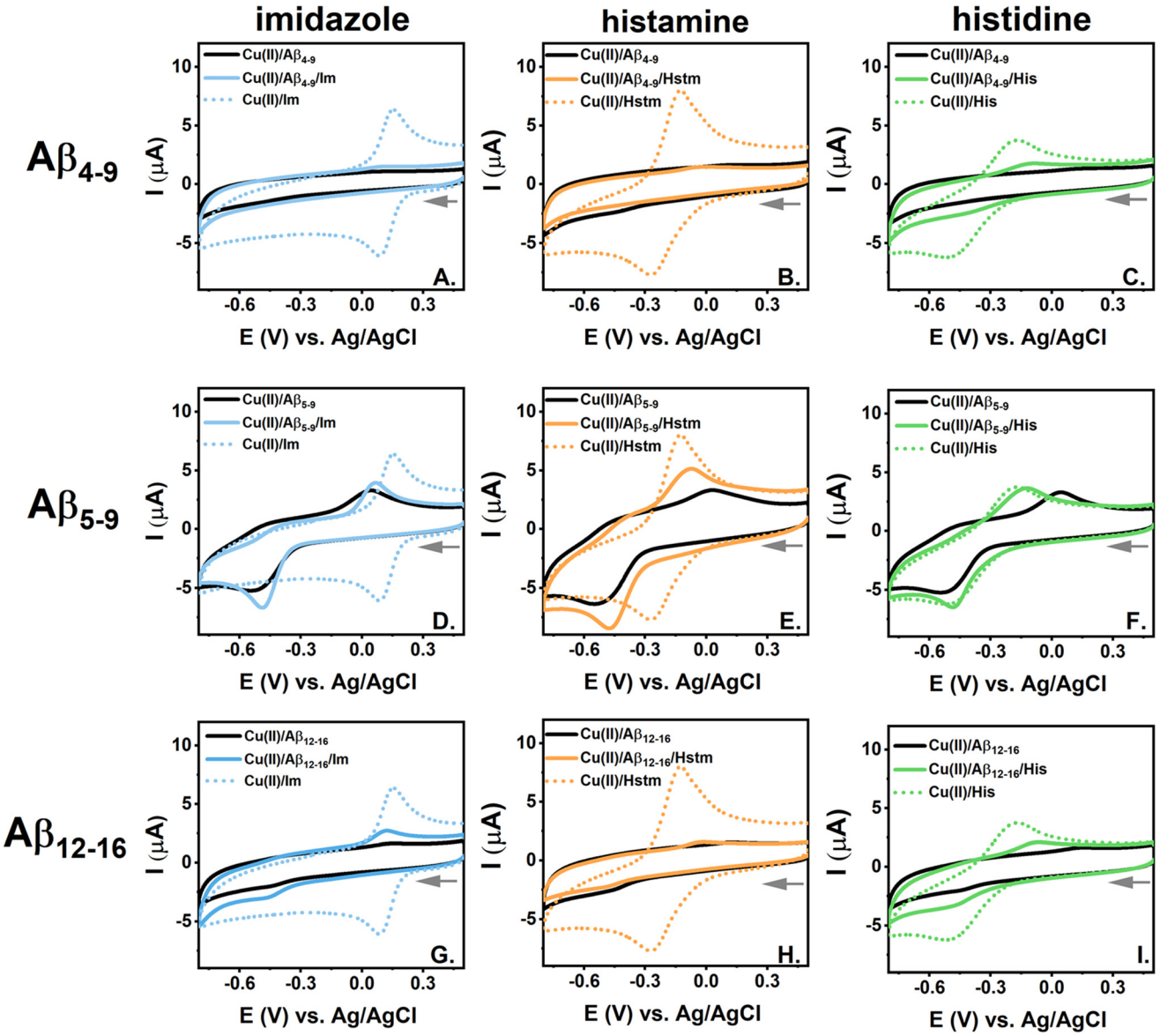

Fig. 4 CV curves recorded scanning towards more negative potential values for ternary systems containing 0.45 mM Cu(II); 0.50 mM Aβ peptides, $Aβ_{4-9}$ (A–C), $Aβ_{5-9}$ (D–F) or $Aβ_{12-16}$ (G–I), and 5.0 mM imidazole (Im) (A, D, G), histamine (Hstm) (B, E, H) or histidine (His) (C, F, I) (blue, orange or green solid lines, respectively). The curves for the corresponding binary systems containing 0.45 mM Cu(II)/0.50 mM Aβ peptides (black lines) and 0.45 mM Cu(II)/5.00 mM imidazole (Im), histamine (Hstm) and histidine (His) (blue, orange or green dotted lines) are shown for comparison. The measurements were performed in 100 mM KNO_3, pH 7.4.

LMW substance and the positive-charged $Aβ_{12-16}$. Both those effects could promote Cu(II) reduction in the Cu(II)/$Aβ_{12-16}$/His system (Fig. 4I), but as shown by the spectroscopic studies, Cu(II) ion removal from Cu(II)/$Aβ_{12-16}$ by histidine prevailed due to the unique stability of the Cu(II) complexes of histidine among the studied Cu(II) complexes of the LMW substances[33] and the relatively tight Cu(II)/$Aβ_{12-16}$ structure.

The picture was more straightforward for the Cu(I) oxidation processes during the reverse CV scans. The signals for the ternary systems with histamine and histidine clearly followed those of the binary Cu(II)/LMW systems (Fig. 4E, F and I). In consequence, the Cu(II)/Cu(I) cycle became far more reversible for the ternary systems of Cu(II)/His-2 peptide with Hstm or His compared to that of the binary Cu(II) complexes of the His-2 peptides. This effect was even more enhanced as the signal for Cu(II) reduction for the 3N complex was shifted slightly towards less negative values in the presence of those LMW molecules. For example, the difference between the Cu(II) reduction and Cu(I) oxidation potential decreased from about 0.58 V for the binary Cu(II)/$Aβ_{5-9}$ complex to about 0.40 V for the ternary system Cu(II)/$Aβ_{5-9}$/Hstm (Fig. 4E).

Cu(II) oxidation in the ternary Cu(II)/Aβ/LMW systems. Analysis of Cu(II) oxidation for the ternary Cu(II)/Aβ/LMW systems was mainly based on the DPV results due to their

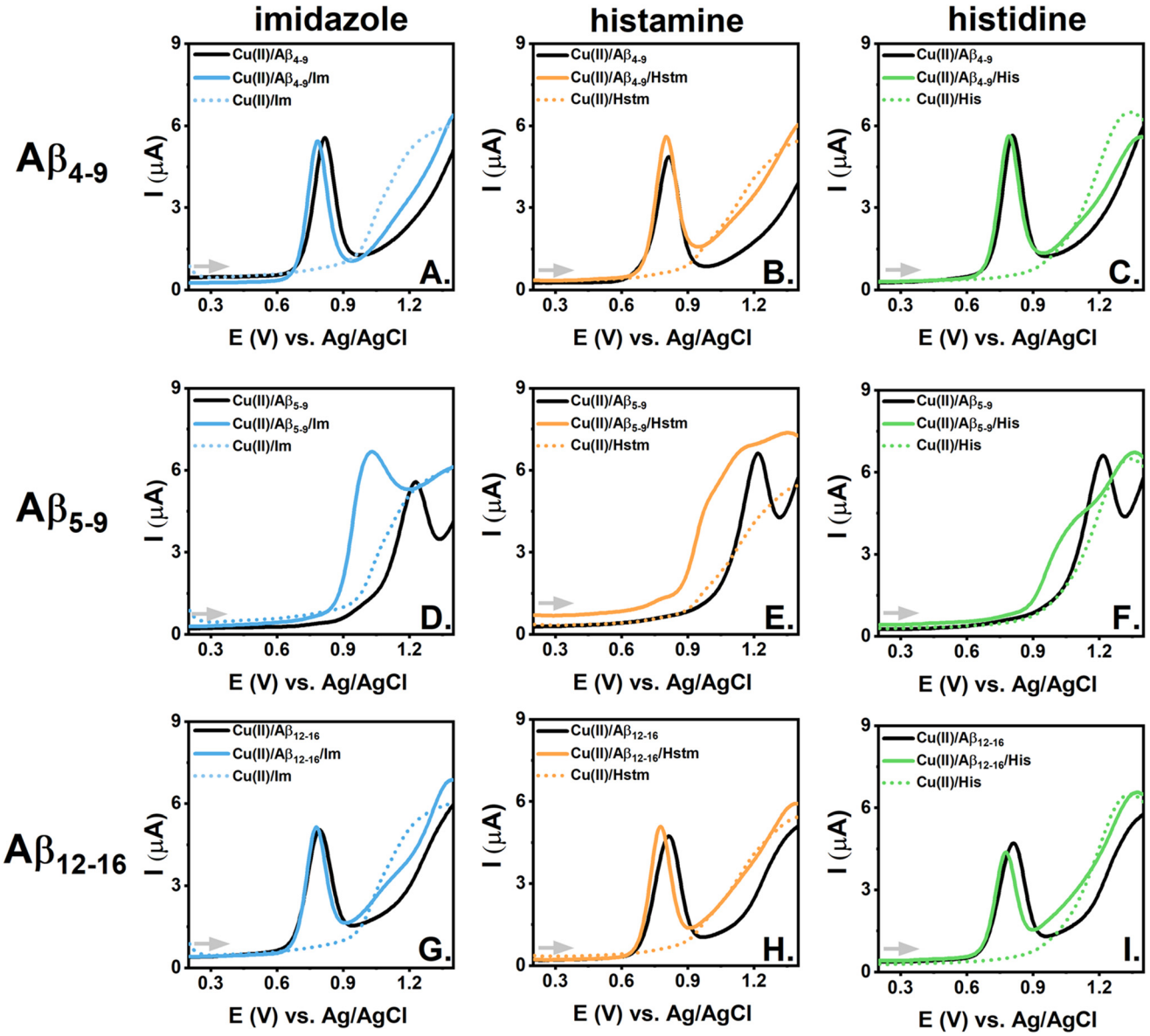

Fig. 5 DPV curves recorded scanning towards more positive potential values for ternary systems containing 0.45 mM Cu(II); 0.50 mM Aβ peptides, $Aβ_{4-9}$ (A–C), $Aβ_{5-9}$ (D–F) or $Aβ_{12-16}$ (G–I), and 5.0 mM imidazole (Im) (A, D, G), histamine (Hstm) (B, E, H) or histidine (His) (C, F, I) (blue, orange or green solid lines, respectively). The curves for the corresponding binary systems containing 0.45 mM Cu(II)/0.50 mM Aβ peptides (black lines) and 0.45 mM Cu(II)/5.00 mM imidazole (Im), histamine (Hstm) and histidine (His) (blue, orange or green dotted lines) are shown for comparison. The measurements were performed in 100 mM KNO_3 at pH 7.4.

better signal separation compared to the CV signals. Comparison of DPV curves of the Cu(II)/Aβ, Cu(II)/LMW, and Cu(II)/Aβ/LMW systems for Cu(II) oxidation is shown in Fig. 5, whereas the respective CV signals are available in Fig. S15.† The electrochemical results in the 0.5–5.0 mM LMW range are given in Fig. S16† for the CV curves, and Fig. S17† for the DPV curves.

The effect of the studied LMW substances on the Cu(II) oxidation signals characteristic for $Aβ_{4-9}$ and $Aβ_{12-16}$ complexes was very subtle. It was associated with a slight shift of the anodic peaks towards less positive values (for the DPV curves, on average about 18 mV *vs.* Ag/AgCl upon the addition of 5 mM LMW substances to Cu(II)/$Aβ_{4-9}$ and about 35 mV *vs.* Ag/AgCl upon the addition of 5 mM LMW substances to Cu(II)/$Aβ_{12-16}$, Fig. 5) and a minor improvement in the Cu(II) oxidation reversibility in both cases (ΔE decreased by about 10 mV, Fig. S15A–C and S15G–I†). Thus, the influence of the studied LMW molecules on Cu(II) oxidation of the $Aβ_{4-9}$ and $Aβ_{12-16}$ complexes was likely limited to the second coordination sphere of the copper-peptide chelates.

A more pronounced impact of LMW substances was noticed for the Cu(II) oxidation of Cu(II)/$Aβ_{5-9}$, as shown in Fig. 5D–F and Fig. S15D–F.† The oxidation potential registered by DPV was about 200 mV lower upon the addition of 5 mM

imidazole to Cu(II)/Aβ$_{5-9}$ (Fig. S15D†). In our previous electrochemical studies on Cu(II) oxidation for His-2 peptide complexes in the presence of imidazole[9,35] and phosphates,[10,11] we also observed a shift of the anodic peak towards less positive values. In such species, imidazole and phosphates fulfil the vacant position in the square-planar Cu(II)/His-2 peptide complex structure, facilitating Cu(II) conversion to the Cu(III) oxidation state. Analysis of the oxidation processes for the ternary Cu(II)/Aβ$_{5-9}$ systems with histamine and histidine is more challenging due to the proximity to the region for imidazole ring oxidation for those LMW compounds (Fig. S15E and F†). A better separation of the signals was achieved by using DPV (Fig. 5D–F) and decreased LMW concentrations (Fig. S17D–F and S18†). For example, considering the ternary Cu(II)/Aβ$_{5-9}$ system with 2.5 mM histamine or 2.5 mM histidine (Fig. S18†), we could estimate that the shift of the Cu(II) oxidation signal upon the addition of those LMW substances to Cu(II)/Aβ$_{5-9}$ was highly depressed compared to the ternary system with imidazole (respectively about 70 mV for histamine and histidine and about 190 mV for imidazole). This aligns with the limited ability of histamine and histidine to create ternary species with Cu(II)/Aβ$_{5-9}$ as proposed in the previous section related to Cu(II) reduction. Moreover, a significant decrease in the current was noticed for the Cu(II)/Aβ$_{5-9}$/His DPV signals compared to for Cu(II)/Aβ$_{5-9}$ (see Fig. S15F, S17F and S18C†), confirming the competitive Cu(II) binding by histidine from Cu(II)/Aβ$_{5-9}$ (Table S3†).

Conclusions

The high stability of Cu(II) complexes with Aβ peptides with His-2 and His-3 motifs suggests that Cu(II) ions preferentially interact with N-truncated peptides rather than other Aβ forms. Moreover, the N-truncated forms, such as Aβ$_{4-x}$, constitute a substantial portion of Aβ peptides in the brain. Thus, any alteration of the redox activity of their Cu(II) complexes could significantly affect the overall status of the potentially toxic copper redox-active species. Employing electrochemical techniques, such as cyclic voltammetry and differential pulse voltammetry, as well as UV–vis spectroscopy, we distinguished various mechanisms for the changes triggered by imidazole-containing low-molecular-weight substances, such as imidazole, histamine, and histidine. The most crucial ones involve (i) competitive Cu(II) binding by LMW substances from the Aβ peptide, creating species more prone to Cu(II) reduction (*i.e.* in the ternary system Cu(II)/Aβ$_{4-9}$/His), (ii) changes in the Cu(II)/Aβ coordination mode triggered by LMW substances, promoting Cu(II) reduction in the Cu(II)/Aβ complexes (*i.e.* in the ternary system Cu(II)/Aβ$_{12-16}$/Im), (iii) Cu(I) reoxidation supported by LMW substances narrowing the distance between the Cu(II) reduction and the Cu(I) oxidation potentials (*i.e.* in the ternary system Cu(II)/Aβ$_{5-9}$/Hstm system). Altogether, these processes favour Cu(II)/Cu(I) cycling, which likely participates in the production of reactive oxygen species and the elevated level of oxidative stress detected in the brain of Alzheimer's disease patients.

Moreover, the oxidation of either Cu(II) or the imidazole ring of LMW molecules was also promoted in the studied ternary Cu(II)/Aβ/LMW systems, especially in those containing the His-2 peptide complexes. But, in contrast to the Cu(II) reduction-related process, the potential values of the oxidation of Cu(II) ions or LMW compounds were still too high to provide a high biological importance. Still, those measurements could serve as valuable information on the Cu(II) complex structure or may be employed in analytical methods for the recognition of LMW substances and Aβ peptides.[10,11]

In view of the substantial effect of LMW compounds on Cu(II)/Cu(I) cycling in N-truncated Aβ complexes, further studies on such systems are highly recommended. More detailed studies on the electron-transfer mechanism in the selected ternary systems, similar to those performed for binary Cu(II)/Aβ$_{1-16}$,[57] are planned to describe how the Cu(II) species are preorganized prior to the redox reaction. Measurements at various pH values could also provide valuable data on such a mechanism, especially for systems in which the LMW substances affect the coordination mode of the Cu(II)/peptide complexes, such as for the ternary systems comprising Aβ$_{12-16}$. The pH dependence has already been described for the electrochemical activity of Cu(II) ions in complexes of Aβ$_{1-16}$,[58] Aβ$_{4-16}$,[59] Aβ$_{3-16}$,[33] Aβ$_{p3-16}$,[33] Aβ$_{11-16}$,[34] Aβ$_{p11-16}$,[34] and here for Aβ$_{12-16}$, but similar studies in ternary systems are missing. It is also worth employing physiological reducing and oxidizing agents to induce the redox reaction instead of initializing it by changes in the electrode potential. Furthermore, methods that are more suitable for a few orders of magnitude lower levels of analytes could better correspond to the physiological Aβ concentration in cerebrospinal fluid,[60] whereas expanding the project by including kinetic measurements could align the latest discoveries regarding the formation of Cu(II) complexes with N-truncated Aβ peptides and other His-3 peptides.[61–63] Therefore, we plan to continue this study considering various effects of LMW substances on the redox activity of the Cu(II)/Aβ complexes demonstrated here by electrochemical methods due to the potential high importance of the obtained results for Alzheimer's disease pathology.

Author contributions

Conceptualization: N. E. W.; experimental supervision: A. T., N. E. W., U. E. W.; instrumental measurements and formal analysis: A. E. J., A. T., N. E. W., A. S.; data processing and visualization: N. E. W., A. T.; writing of the original draft: N. E. W.; writing – review & editing: all authors; funding acquisition and resources: N. E. W., W. W. All authors have given approval to the final version of the manuscript.

Data availability

The data supporting this article have been included as part of the ESI.†

Conflicts of interest

There are no conflicts to declare.

Acknowledgements

This work has been financially supported by the Warsaw University of Technology under the Program Excellence Initiative, Research University (ID-UB), BIOTECHMED-1 Project No. PSP 504/04496/1020/45.010407.

References

1 A. Association, *Alzheimer's Dementia*, 2023, **19**, 1598–1695.
2 M. A. Smith, *Int. Rev. Neurobiol.*, 1998, **42**, 1–54.
3 G. G. Glenner and C. W. Wong, *Biochem. Biophys. Res. Commun.*, 1984, **120**, 885–890.
4 E. Pham, L. Crews, K. Ubhi, L. Hansen, A. Adame, A. Cartier, D. Salmon, D. Galasko, S. Michael, J. N. Savas, J. R. Yates, C. Glabe and E. Masliah, *FEBS J.*, 2010, **277**, 3051–3067.
5 C. Cheignon, M. Jones, E. Atrián-Blasco, I. Kieffer, P. Faller, F. Collin and C. Hureau, *Chem. Sci.*, 2017, **8**, 5107–5118.
6 E. Portelius, N. Bogdanovic, M. K. Gustavsson, I. Volkmann, G. Brinkmalm, H. Zetterberg, B. Winblad and K. Blennow, *Acta Neuropathol.*, 2010, **120**, 185–193.
7 E. Stefaniak and W. Bal, *Inorg. Chem.*, 2019, **58**, 13561–13577.
8 M. Mital, N. E. Wezynfeld, T. Frączyk, M. Z. Wiloch, U. E. Wawrzyniak, A. Bonna, C. Tumpach, K. J. Barnham, C. L. Haigh, W. Bal and S. C. Drew, *Angew. Chem., Int. Ed.*, 2015, **54**, 10460–10464.
9 N. E. Wezynfeld, A. Tobolska, M. Mital, U. E. Wawrzyniak, M. Z. Wiloch, D. Płonka, K. Bossak-Ahmad, W. Wróblewski and W. Bal, *Inorg. Chem.*, 2020, **59**, 14000–14011.
10 A. Tobolska, N. E. Wezynfeld, U. E. Wawrzyniak, W. Bal and W. Wróblewski, *Dalton Trans.*, 2021, **50**, 2726–2730.
11 A. Tobolska, K. Głowacz, P. Ciosek-Skibińska, W. Bal, W. Wróblewski and N. E. Wezynfeld, *Dalton Trans.*, 2022, **51**, 18143–18151.
12 A. Tobolska, N. E. Wezynfeld, U. E. Wawrzyniak, W. Bal and W. Wróblewski, *Chem. Proc.*, 2021, **5**, 39.
13 C. Cheignon, F. Collin, L. Sabater and C. Hureau, *Antioxidants*, 2023, **12**, 472.
14 M. Z. Wiloch, U. E. Wawrzyniak, I. Ufnalska, A. Bonna, W. Bal, S. C. Drew and W. Wróblewski, *J. Electrochem. Soc.*, 2016, **163**, G196–G199.
15 M. Mital, W. Bal, T. Frączyk and S. C. Drew, *Inorg. Chem.*, 2018, **57**, 6193–6197.
16 K. Bossak-Ahmad, M. Mital, D. Płonka, S. C. Drew and W. Bal, *Inorg. Chem.*, 2019, **58**, 932–943.
17 P. Gonzalez, B. Vileno, K. Bossak, Y. El Khoury, P. Hellwig, W. Bal, C. Hureau and P. Faller, *Inorg. Chem.*, 2017, **56**, 14870–14879.
18 S. Mena, A. Mirats, A. B. Caballero, G. Guirado, L. A. Barrios, S. J. Teat, L. Rodriguez-Santiago, M. Sodupe and P. Gamez, *Chem. – Eur. J.*, 2018, **24**, 5153–5162.
19 P. Gonzalez, K. Bossak-Ahmad, B. Vileno, N. E. Wezynfeld, Y. El Khoury, P. Hellwig, C. Hureau, W. Bal and P. Faller, *Chem. Commun.*, 2019, **55**, 8110–8113.
20 B. Alies, E. Renaglia, M. Rózga, W. Bal, P. Faller and C. Hureau, *Anal. Chem.*, 2013, **85**, 1501–1508.
21 K. Bossak, M. Mital, J. Poznański, A. Bonna, S. Drew and W. Bal, *Inorg. Chem.*, 2016, **55**, 7829–7831.
22 H. L. Haas, O. A. Sergeeva and O. Selbach, *Physiol. Rev.*, 2008, **88**, 1183–1241.
23 M. B. Passani, P. Panula and J. S. Lin, *Front. Syst. Neurosci.*, 2014, **8**, 64.
24 A. Satpati, T. Neylan and L. T. Grinberg, *Alzheimer's Dement.: Transl. Res. Clin. Interv.*, 2023, **9**, e12379.
25 L. Fernández-Novoa and R. Cacabelos, *Behav. Brain Res.*, 2001, **124**, 213–233.
26 I. M. Mazurkiewicz-Kwilecki and S. Nsonwah, *Can. J. Physiol. Pharmacol.*, 1989, **67**, 75–78.
27 P. Panula, J. Rinne, K. Kuokkanen, K. Eriksson, T. Sallmen, H. Kalimo and M. Relja, *Neuroscience*, 1997, **82**, 993–997.
28 J. D. Brioni, T. A. Esbenshade, T. R. Garrison, S. R. Bitner and M. D. Cowart, *J. Pharmacol. Exp. Ther.*, 2011, **336**, 38.
29 A. N. Fonteh, R. J. Harrington, A. Tsai, P. Liao and M. G. Harrington, *Amino Acids*, 2007, **32**, 213–224.
30 N. Elgrishi, K. J. Rountree, B. D. McCarthy, E. S. Rountree, T. T. Eisenhart and J. L. Dempsey, *J. Chem. Educ.*, 2018, **95**, 197–206.
31 C. Hureau, V. Balland, Y. Coppel, P. L. Solari, E. Fonda and P. Faller, *J. Biol. Inorg. Chem.*, 2009, **14**, 995–1000.
32 S. Timári, R. Cerea and K. Várnagy, *J. Inorg. Biochem.*, 2011, **105**, 1009–1017.
33 M. Z. Wiloch, N. Baran and M. Jönsson-Niedziółka, *ChemElectroChem*, 2022, **9**, e202200623.
34 M. Z. Wiloch and M. Jönsson-Niedziółka, *J. Electroanal. Chem.*, 2022, **922**, 116746.
35 I. Ufnalska, U. E. Wawrzyniak, K. Bossak-Ahmad, W. Bal and W. Wróblewski, *J. Electroanal. Chem.*, 2020, **862**, 1–10.
36 A. Tobolska, N. E. Wezynfeld, U. E. Wawrzyniak, W. Bal and W. Wróblewski, *Inorg. Chem.*, 2021, **60**, 19448–19456.
37 W. C. Chan and P. D. White, *Fmoc Solid Phase Peptide Synthesis*, 2000.
38 M. Mital, J. P. Sęk and Z. M. Ziora, in *Peptide Synthesis: Methods and Protocols*, ed. W. M. Hussein, M. Skwarczynski and I. Toth, Springer, US, New York, NY, 2020, pp. 323–336.
39 P. Gonzalez, K. Bossak, E. Stefaniak, C. Hureau, L. Raibaut, W. Bal and P. Faller, *Chem. – Eur. J.*, 2018, **24**, 8029–8041.
40 A. G. Al-Harazie, E. A. Gomaa, R. R. Zaky and M. N. Abd El-Hady, *ACS Omega*, 2023, **8**, 13605–13625.
41 C. Esmieu, G. Ferrand, V. Borghesani and C. Hureau, *Chem. – Eur. J.*, 2021, **27**, 1777–1786.
42 F. Kracke, I. Vassilev and J. O. Krömer, *Front. Microbiol.*, 2015, **6**, 575.

43 C. Hureau, H. Eury, R. Guillot, C. Bijani, S. Sayen, P. L. Solari, E. Guillon, P. Faller and P. Dorlet, *Chem. – Eur. J.*, 2011, **17**, 10151–10160.
44 P. Deschamps, P. P. Kulkarni, M. Gautam-Basak and B. Sarkar, *Coord. Chem. Rev.*, 2005, **249**, 895–909.
45 I. Török, T. Gajda, B. Gyurcsik, G. K. Tóth and A. Péter, *J. Chem. Soc., Dalton Trans.*, 1998, 1205–1212.
46 R. J. Sundberg and R. B. Martin, *Chem. Rev.*, 1974, **74**, 471–517.
47 G. Brookes and L. D. Pettit, *J. Chem. Soc., Dalton Trans.*, 1976, 1224.
48 H.-L. Wang, R. M. O'malley and J. E. Fernandez, *Macromolecules*, 1994, **27**, 893–901.
49 P. Puthongkham, S. T. Lee and B. J. Venton, *Anal. Chem.*, 2019, **91**, 8366–8373.
50 L. C. Chen, C. C. Chang and H. C. Chang, *Electrochim. Acta*, 2008, **53**, 2883–2889.
51 K. Bossak-Ahmad, M. D. Wiśniewska, W. Bal, S. C. Drew and T. Frączyk, *Int. J. Mol. Sci.*, 2020, **21**, 6190.
52 R. Kotuniak, T. Frączyk, P. Skrobecki, D. Płonka and W. Bal, *Inorg. Chem.*, 2018, **57**, 15507–15516.
53 A. Santoro, G. Walke, B. Vileno, P. P. Kulkarni, L. Raibaut and P. Faller, *Chem. Commun.*, 2018, **54**, 11945–11948.
54 A. Santoro, N. E. Wezynfeld, M. Vašák, W. Bal and P. Faller, *Chem. Commun.*, 2017, **53**, 11634–11637.
55 E. Stefaniak, D. Płonka, P. Szczerba, N. E. Wezynfeld and W. Bal, *Inorg. Chem.*, 2020, **59**, 4186–4190.
56 P. Gonzalez, L. Sabater, E. Mathieu, P. Faller and C. Hureau, *Biomolecules*, 2022, **12**, 1327.
57 V. Balland, C. Hureau and J.-M. Savéant, *Proc. Natl. Acad. Sci. U. S. A.*, 2010, **5**, 17113–17118.
58 L. Rivillas-Acevedo, R. Grande-Aztatzi, I. Lomelí, J. E. García, E. Barrios, S. Teloxa, A. Vela and L. Quintanar, *Inorg. Chem.*, 2011, **50**, 1956–1972.
59 M. Z. Wiloch, S. Linfield, N. Baran, W. Nogala and M. Jönsson-Niedziółka, *Electrochim. Acta*, 2024, **485**, 144089.
60 T. Skillbäck, B. Y. Farahmand, C. Rosén, N. Mattsson, K. Nägga, L. Kilander, D. Religa, A. Wimo, B. Winblad, J. M. Schott, K. Blennow, M. Eriksdotter and H. Zetterberg, *Brain*, 2015, **138**, 2716–2731.
61 R. Kotuniak, M. J. F. Strampraad, K. Bossak-Ahmad, U. E. Wawrzyniak, I. Ufnalska, P.-L. Hagedoorn and W. Bal, *Angew. Chem.*, 2020, **59**, 11234–11239.
62 X. Teng, E. Stefaniak, P. Girvan, R. Kotuniak, D. Płonka, W. Bal and L. Ying, *Metallomics*, 2020, **12**, 470–473.
63 R. Kotuniak and W. Bal, *Metallomics*, 2023, **15**, mfad007.